Systems/Circuits

Kappa Opioid Receptors Mediate Heterosynaptic Suppression of Hippocampal Inputs in the Rat Ventral Striatum

Julie M. Brooks and ⊕**Patricio O'Donnell**

Neuroscience and Pain Research Unit, Pfizer, Cambridge, Massachusetts 02139

Kappa opioid receptors (KORs) are highly enriched within the ventral striatum (VS) and are thought to modulate striatal neurotransmission. This includes presynaptic inhibition of local glutamatergic release from excitatory inputs to the VS. However, it is not known which inputs drive this modulation and what impact they have on the local circuit dynamics within the VS. Individual medium spiny neurons (MSNs) within the VS serve as a site of convergence for glutamatergic inputs arising from the PFC and limbic regions, such as the hippocampus (HP). Recent data suggest that competition can arise between these inputs with robust cortical activation leading to a reduction in ongoing HP-evoked MSN responses. Here, we investigated the contribution of KOR signaling in PFC-driven heterosynaptic suppression of HP inputs onto MSNs using whole-cell patch-clamp recordings in slices from adult rats. Optogenetically evoked HP EPSPs were greatly attenuated after a short latency (50 ms) following burst-like PFC electrical stimulation, and the magnitude of this suppression was partially reversed following blockade of GABA$_A$Rs (GABA Type A receptors), but not GABA$_B$Rs (GABA Type B receptors). A similar reduction in suppression was observed in the presence of the KOR antagonist, norBNI. Combined blockade of local GABA$_A$Rs and KORs resulted in complete blockade of PFC-induced heterosynaptic suppression of less salient HP inputs. These findings highlight a mechanism by which strong, transient PFC activity can take precedence over other excitatory inputs to the VS.

Key words: dynorphin; kappa opioid receptor; medium spiny neurons; nucleus accumbens; ventral striatum; whole-cell patch-clamp

---

Significance Statement

Emerging evidence suggests that kappa opioid receptor (KOR) activation can selectively modulate striatal glutamatergic inputs onto medium spiny neurons (MSNs). In this study, we found that robust cortical stimulation leads to a reduction in ongoing hippocampal-evoked MSNs responses through the combined recruitment of local inhibitory mechanisms and activation of pre-synaptic KORs in the ventral striatum (VS). These processes are likely to facilitate the efficient transfer of cortical information through the VS during critical decision making by dampening competing information from less salient excitatory inputs. These data provide a novel mechanism through which VS information processing could influence decision making, a function thought to occur primarily in the PFC.

Introduction

The κ opioid receptor (KOR) system is implicated in the regulation of neurotransmitter release in the ventral striatum (VS). Both KOR and its endogenous ligand, the dynorphin (DYN) peptide, are highly enriched throughout the VS (Fallon and Leslie, 1986; Mansour et al., 1994). DYN is preferentially expressed in axonal processes of GABAergic medium spiny projection neu-

rons (MSNs) that express D1 DA receptors (Altar and Hauser, 1987). In addition, electron microscopy studies indicate that KORs are located presynaptically on midbrain dopaminergic terminals directly opposing the DA transporter, as well as on asymmetric, presumably glutamatergic inputs (Svingos et al., 1999; Meshul and McGinty, 2000). The role of these receptors on information processing within the VS remains unclear.

The effects of KOR agonists within the VS are thought to occur primarily through presynaptic control of neurotransmitter release. Most studies to date have focused primarily on KOR regulation of DA release; it has been shown that presynaptic activation of KORs on DA inputs exerts profound inhibitory control over striatal DA signaling (Di Chiara and Imperato, 1988; Spanagel et al., 1992; Ebner et al., 2010). However, striatal KORs are also present on presynaptic terminals of presumed excitatory synapses (Svingos et al., 1999; Meshul and McGinty, 2000), yet

few studies have investigated the impact of KORs on excitatory neurotransmission and local circuit dynamics within the VS. Consistent with this anatomical localization, synaptosomal (Rawls and McGinty, 1998; Hill and Brotchie, 1999; Rawls et al., 1999) and *in vitro* electrophysiology studies (Hjelmstad and Fields, 2001, 2003) revealed that administration of the KOR agonist U69,593 reduces presynaptic glutamatergic neurotransmission in the VS. Furthermore, emerging evidence suggests KOR activation selectively modulates BLA excitatory input onto D1 MSNs (Tejeda et al., 2017). However, the BLA provides only a portion of the excitatory inputs to the VS. It is not known what inputs activate KOR-dependent mechanisms and how input-driven KOR activation shapes information integration in this region.

The VS receives significant excitatory glutamatergic inputs from several cortical and subcortical brain regions, including the PFC (Fallon and Leslie, 1986; Berendse et al., 1992) and hippocampus (HP) (Groenewegen et al., 1999). These afferent inputs converge onto individual VS MSNs (O'Donnell and Grace, 1995; French and Totterdell, 2002) and interact nonlinearly. Previous conceptualizations surrounding their interaction emphasized the importance of HP inputs acting as a gating mechanism for information flow through the VS (O'Donnell and Grace, 1995). However, more recent data suggest that these functionally distinct excitatory inputs may differentially influence striatal circuitry in an activity-dependent manner. For example, electrophysiological recordings from anesthetized rats revealed that robust PFC stimulation leads to a reduction in ongoing HP-evoked MSN responses, in part, through the recruitment of local inhibitory mechanisms (Calhoon and O'Donnell, 2013). Therefore, it is possible that burst-like PFC activity is capable of attenuating weaker, competing excitatory input locally within the striatum.

KOR modulation of glutamatergic inputs to the VS provides a potential mechanism by which robust PFC activation could impact the efficacy of competing excitatory inputs onto an individual MSN. Here, we investigated the contribution of KOR/DYN signaling in PFC-driven heterosynaptic suppression of HP inputs onto MSNs in the VS. Input interactions between electrical stimulation of corticostriatal fiber tracts and optogenetic stimulation of HP inputs expressing channelrhodopsin were tested in VS MSNs using whole-cell patch-clamp recordings in slices from adult rats.

Materials and Methods

Subjects. Adult male Sprague Dawley rats (350–450 g; Charles River Laboratory) served as subjects for all experiments. Rats were maintained in a temperature- and humidity-controlled environment on a 12 h light/dark cycle (lights on at 6:30 A.M.) with food and water available *ad libitum*. Animal care and experimentation were performed in accordance with protocols approved by the University of Maryland School of Medicine and Pfizer Institutional Animal Care and Use Committees, consistent with the National Institutes of Health's *Guide for the care and use of laboratory animals*.

Optogenetic techniques. Rats were anesthetized with inhalant isoflurane (3%, 0.8 L/min, O_2). An adeno-associated viral vector (serotype 5) expressing channelrhodopsin2-eYFP (ChR2) under the CamKinase II promotor was bilaterally infused into the ventral HP (Fig. 1A; 5.8 mm caudal to bregma; ±4.7 mm lateral from midline, and at depths of 8.0, 7.0, and 4.0 mm from surface; 0.5 μl/injection site) at a rate of 0.15 μL/min using a Hamilton syringe pump. *In vitro* electrophysiology recording experiments were performed 6–8 weeks following surgery. ChR2 transfection was assessed using eYFP fluorescence detection at the recording site (Fig. 1B). Optical stimulation of transfected HP terminals was evoked using a single 470 nm wavelength light pulse (8–10 mW, 1 ms) generated via a Lambda LS illuminator controlled by a Lambda10-B filter wheel (Sutter Instruments) delivered through a 40× objective.

Electrophysiology. Rats were anesthetized with chloral hydrate (400 mg/kg, i.p.) or isoflurane (3%, 0.8 L/min, O_2) and transcardially perfused before decapitation with oxygenated ice-cold aCSF (in mM) as follows: 125 NaCl, 25 NaHCO$_3$, 10 glucose, 3.5 KCl, 1.25 NaH$_2$PO$_4$, 0.5 CaCl$_2$, 3 MgCl$_2$, pH 7.4, osmolarity 295 mOsm, constantly oxygenated with 95% O_2 and 5% CO_2. Parasagittal slices (300 μm thick) containing the VS and corticostriatal fibers were sectioned using a 10° angle (midline face up and caudal end lifted) on a Vibratome. Slices were incubated in oxygenated aCSF warmed to ~34°C for at least 1 h before recording. For each experiment, slices were placed in a submersion-type recording chamber superfused with oxygenated aCSF at a flow rate of 2 mL/min and maintained at 33°C-34°C. Recording aCSF was adjusted to include 2 mM CaCl$_2$ and 1 mM MgCl$_2$.

Whole-cell current-clamp recordings were performed from MSNs in both the shell and core regions of the NAc within the VS in brain slices obtained from adult rats between 1.40 and 2.1 mm lateral from midline. These sections were selected based on the combined presence of corticostriatal fiber tracts and robust ChR2-eYFP expression. Cells were identified using infrared differential interference contrast microscopy (Olympus BX50-WI) using a 40× water-immersion objective. Visual guidance was obtained with an infrared-sensitive CCD camera (DAGE-MTI) connected to a monitor. Patch pipettes (6–10 MΩ) were made from 1.5 mm OD borosilicate glass tubing (World Precision Instruments) filled with the following (in mM): 115 K-gluconate, 10 HEPES, 2 MgCl$_2$, 20 KCL, 2 Mg-ATP, 2 Na$_2$-ATP, and 0.3 GTP, pH 7.3; osmolarity 280 mOsm. Neurobiotin (0.125%) was added to the internal recording solution for histological identification of recorded cells. Whole-cell recordings were acquired with a computer-controlled Multiclamp 700B amplifier (Molecular Devices), digitized (Digidata, Molecular Devices), and sampled with Axoscope 9.0 (Molecular Devices) at a rate of 10 kHz. Electrode potentials were adjusted to zero before recording without correcting the liquid junction potential.

Stimulation protocols. Recording sessions began with a brief stabilization period followed by a full assessment of passive membrane properties, including membrane potential and input resistance (measured using the slope of a current–voltage plot obtained with 500 ms hyperpolarizing and depolarizing pulses). Neurons exhibiting a resting membrane potential more depolarized than −70 mV, spike amplitudes <70 mV from threshold, and/or an input resistance <80 MΩ were excluded from analysis. Optical and electrical stimuli were controlled using a Master 8 pulse generator (A.M.P.I.). Cortical synaptic responses were evoked using a bipolar electrode made from a twisted pair of Teflon-coated tungsten wires (tips ~200 μm apart). The electrode was placed within the forceps minor, ~500 μm from the recorded cell.

To determine the effect of burst-like PFC stimulation on striatal MSN responses to ongoing HP input, changes in MSN EPSPs evoked via HP and cortical stimulation were assessed using the following protocol. Recordings began with a baseline optical stimulation of transfected HP terminals (HP1) using a single pulse of 475 nm wavelength of light (8–10 mW; 1 ms). Following a 500 ms delay, a burst-like electrical stimulation was applied to the corticostriatal fiber bundles (five 0.1–0.5 nA, 0.5 ms pulses at 20 Hz). Stimulation intensity was selected for each cell to be subthreshold to firing. Subsequent to the last pulse of the PFC stimulation train, a second test HP stimulus (HP2) was evoked using the same stimulation parameters established for HP1 at varying time delays (50 and 500 ms intervals relative to the end of the PFC stimulation). The order in which the HP2 time delays were presented was counterbalanced across cells. This stimulation protocol (HP1-PFC-HP2; Fig. 1C) was repeated 15 times at 0.066 Hz for each delay interval before and after bath application of drugs. To determine whether changes in HP2 responses were dependent on PFC stimulation, some cells were subjected to the same stimulation protocol as described above but omitting the PFC stimulation (HP1-HP2; Fig. 1C). Following baseline HP1-PFC-HP2, each cell also received direct depolarizing current injection. Target membrane potentials were adjusted so that values at HP1 were comparable with those at HP2 following PFC stimulation during baseline conditions. Finally, for those experiments assessing input specificity of KOR activation, we compared changes in EPSPs evoked via a single HP and PFC stimulation occurring 500 ms apart within the same cell. Values for each
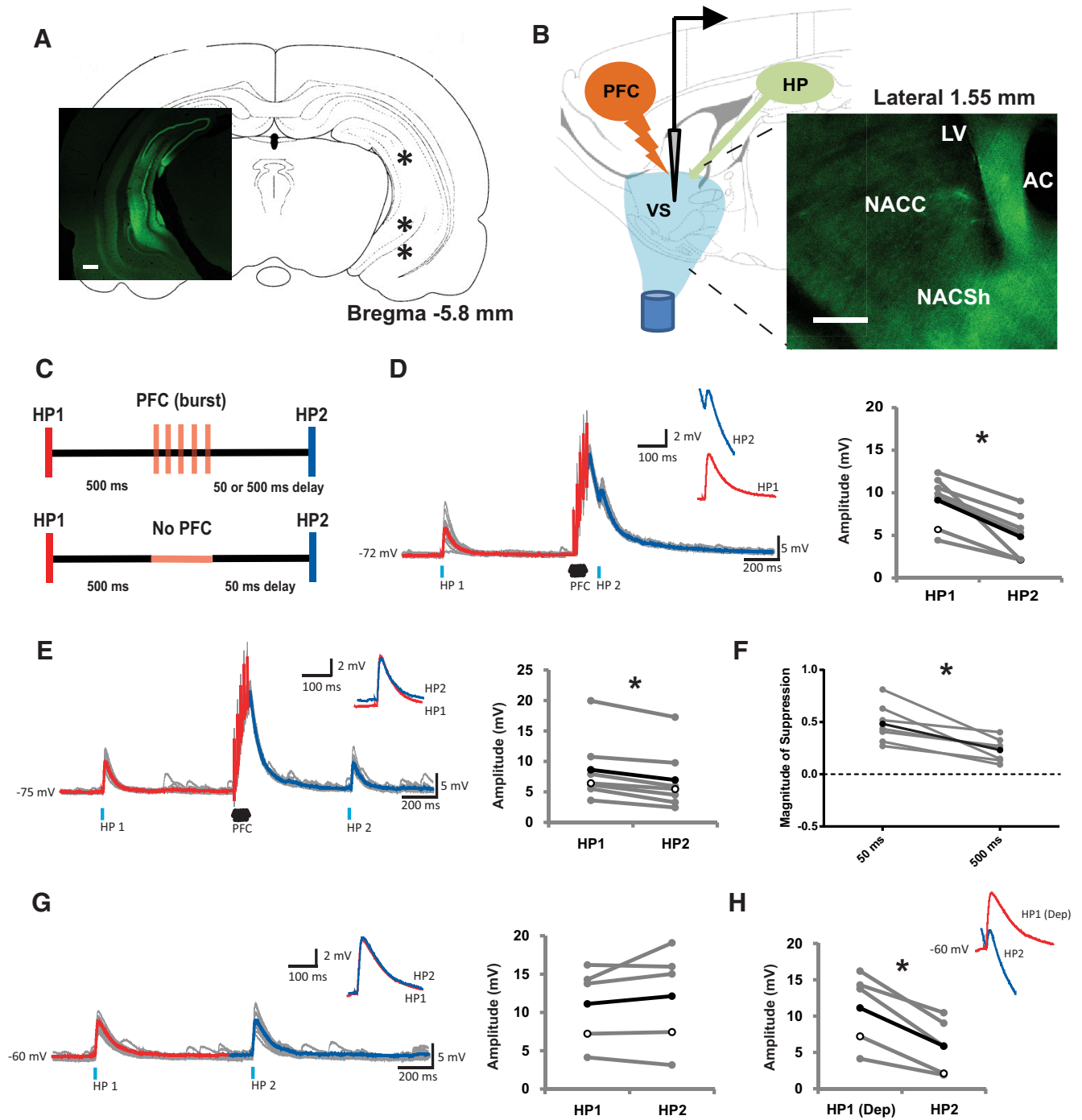
Figure 1. Burst-like stimulation of corticostriatal fibers suppresses optogenetically evoked HP responses in MSNs in acute slices. ***A***, Left, Representative image of ChR2-YFP expression at the injection site (green). Scale bar, 500 μm. Right, Location of bilateral ChR2 injection sites in the VH of rats (*). ***B***, Schematic of striatal MSN recordings conducted using a parasagittal slice orientation. PFC responses were evoked via electrical stimulation of corticostriatal fiber tracks, and HP responses were evoked using a 475 nm wavelength light pulse applied to ChR2-transfected terminals in the VS. Inset, Representative photomicrograph of ChR2-YFP-labeled HP terminals in the VS. Scale bar, 200 μm. ***C***, Top, Stimulation protocol used to study heterosynaptic interactions between HP and PFC inputs to the VS. Bottom, Protocol in which PFC stimulation was omitted before the short (50 ms) HP2 delay period. ***D***, Traces showing response to optogenetic stimulation of HP terminals before (HP1) and 50 ms after (HP2) PFC train stimulation in a representative MSN. Highlighted trace represents the average of the 15 overlaid sweeps shown in gray. Red represents MSN responses occurring before and throughout the PFC stimulation. Blue represents responses occurring after PFC stimulation. Inset, Averaged responses to HP1 and HP2 (highlighted in red and blue, respectively) are enlarged and overlaid. Right, Gray represents averaged EPSP amplitudes for individual MSNs. HP2 responses are significantly reduced compared with HP1 at a short latency following PFC stimulation. Open black symbols represent data from the cell whose traces are illustrated. Closed black symbols represent group averages. ***E***, Responses to optogenetic stimulation of HP terminals before and 500 ms after PFC train stimulation in the same representative MSN. Right, Averaged EPSP amplitudes for individual MSNs showing that HP2 responses remain reduced compared with HP1 at a long latency following PFC stimulation. ***F***, Plot comparing the magnitude of HP2 suppression at 50 or 500 ms following PFC stimulation for individual MSNs. The magnitude of heterosynaptic suppression of HP2 is significantly greater at the shorter (50 ms) delay period. ***G***, Responses to optogenetic stimulation of HP terminals when PFC stimulation is omitted. Right, Averaged EPSP amplitudes for individual MSNs showing that HP1 and HP2 responses are similar when PFC stimulation is omitted. ***H***, Averaged EPSP amplitudes for individual MSNs showing that HP2 EPSPs are still significantly reduced compared with HP1 responses evoked at a similar membrane potential. Inset, Averaged depolarized HP1 and basal HP2 EPSPs in a representative MSN. AC, Anterior commissure; LV, lateral ventricle; NACC, nucleus accumbens core; NACSh, nucleus accumbens shell. *$p < 0.05$.

parameter across all experiments were calculated by averaging evoked responses over all repetitions for each time delay.

All drugs were applied by bath perfusion. Solutions were prepared fresh the day of recording and diluted in recording aCSF to the final concentration. Stock solutions of picrotoxin (PTX) and AM251 were dissolved in DMSO, and the maximal final DMSO concentration was 0.1% (v/v). U69,593 stock solution was diluted in 50% ethanol. Stock solutions of saclofen (SAC) and nor-binaltrophimine (norBNI) were dissolved in recording aCSF. All drugs were purchased from Sigma.

Histological procedures. At the end of each experiment, all slices were placed in 4% PFA overnight. Slices were then washed in 0.1 M PBS and incubated with 0.3% Triton X-100 in PBS. To block endogenous peroxidases, slices were incubated for 15 min in 0.3% hydrogen peroxide. The avidin-biotin complex method was used to detect Neurobiotin-filled cells (ABC peroxidase kit; Vector Laboratories), and the reaction was visualized using DAB (Sigma) to provide verification of the morphology and location of recorded neurons.

Experimental design and statistical analysis. All recordings were conducted using a "within-cell" experimental design, which allowed each cell to serve as its own control and reduced cross cell variability between test conditions. As such, effects of drug treatment and HP2 time delays (50 and 500 ms after PFC stimulation) could be assessed using paired statistical tests. Only one cell was recorded from each brain slice. For each experiment, slices were generated from 5 to 7 adult male Sprague Dawley rats. Exact cell/rat sample sizes are noted alongside corresponding experiments in Results.

Data are expressed as mean ± SD. All analyses were conducted using Prism statistical software version 6.0 (Graphpad Software). Initial heterosynaptic suppression data were analyzed using repeated-measures ANOVA with pulse type (HP1 or HP2) and HP2 delay (50 or 500 ms) as within-subject factors. For each drug treatment condition, the main effects of drug treatment (baseline or compound) and pulse type (HP1 or HP2 at 50 ms delay) were assessed as within-subject factors using repeated-measures ANOVAs. When appropriate, a minimum number of *post hoc* comparisons were conducted using Bonferroni-corrected paired t tests. The magnitude of suppression was calculated by determining the ratio of the control and test pulse amplitudes (HP2/HP1). Given that this value represents the remaining HP2 EPSP amplitude following PFC stimulation compared with HP1 EPSPs, the difference between 1 and HP2/HP1 was reported.

Results

Burst-like stimulation of corticostriatal fibers suppresses optogenetically evoked HP responses in MSNs

To determine whether *in vivo* observations of PFC-driven heterosynaptic suppression of HP inputs onto striatal MSNs (Calhoon and O'Donnell, 2013) could be replicated in an *in vitro* preparation, changes in MSN response to optical stimulation of HP terminals were measured before (HP1) and at varying times after (HP2; 50 or 500 ms) burst-like electrical stimulation delivered to corticostriatal fiber tracts ($n = 7$ cells from 6 rats). Similar to our previous *in vivo* study, burst-like PFC stimulation significantly reduced optically evoked HP2 EPSPs relative to baseline responses (HP1) (Fig. 1D,E; pulse: $F_{(1,6)} = 54.10$; $p = 0.0003$, ANOVA) in a time-dependent manner (pulse $\times$ delay: $F_{(1,6)} = 6.92$; $p = 0.039$, ANOVA). Although cortical stimulation reduced HP2 EPSPs at each time interval, further analysis revealed that the magnitude of suppression induced by PFC activity differed significantly between the two delay periods (Fig. 1F; $t_{(6)} = 4.08$; $p = 0.007$, paired t test). Specifically, HP2 stimuli occurring 50 ms following the end of PFC stimulation were reduced by 48.3 ± 17.4% compared with a 23.3 ± 10.4% reduction of HP2 stimuli occurring 500 ms after PFC activation.

Given the relatively short time interval separating HP1 and HP2 responses at the 50 ms delay period, it is possible that attenuation of HP2 EPSPs is the result of short-term depression and occurred in-

dependent of robust PFC stimulation. To assess this possibility, the 50 ms delay stimulation protocol was run with the PFC stimulation omitted in a subset of cells ($n = 5$ cells). No differences were observed between HP1 and HP2 EPSP amplitudes (Fig. 1G; $t_{(4)} = 1.00$; $p = 0.376$, paired t test), indicating the observed suppression is not an effect of pairing HP pulses and suggesting that burst-like PFC stimulation is a key factor driving HP suppression.

While strong cortical activation significantly reduced the impact of HP inputs onto MSNs, this effect could be the result of voltage-dependent changes in ionic conductances associated with the depolarization driven by cortical stimulation. To determine whether PFC-induced depolarization contributed to the heterosynaptic suppression of HP inputs, responses were compared when HP1 and HP2 were evoked at similar membrane potentials in a subset of cells ($n = 5$). This was accomplished by depolarizing the cell with direct intracellular current injection. Target membrane potentials were adjusted across cells so that values were comparable with those elicited by the PFC stimulus during baseline conditions. Even when evaluated at the same membrane potential, the amplitude of HP2 EPSPs was significantly reduced compared with depolarized HP1 EPSPs (Fig. 1H; $t_{(4)} = 5.02$; $p = 0.007$, paired t test). These data indicate that PFC-driven suppression is not the direct result of depolarization-induced changes in membrane physiology. All subsequent HP2/HP1 comparisons were analyzed when both HP EPSPs were evoked at similar membrane potentials. Our findings support the *in vivo* observation that robust activation of corticostriatal inputs to the VS reduces the potency of less salient HP inputs onto MSNs.

Local GABA$_A$, but not GABA$_B$, inhibition contributes to PFC-induced heterosynaptic suppression in the VS

Based on our *in vivo* study showing that blockade of GABA$_A$Rs partially restores HP EPSPs (Calhoon and O'Donnell, 2013), we hypothesized that local inhibitory signaling contributes to PFC-induced heterosynaptic suppression in the VS. To determine whether a similar GABAergic mechanism is recruited in an *in vitro* preparation, MSN responses to the HP1-PFC-HP2 protocol were measured in the presence of the GABA$_A$ open-channel blocker PTX (100 μM; $n = 7$ cells/6 rats). In the presence of PTX, HP2 EPSPs evoked 50 ms after PFC stimulation remained suppressed compared with HP1 responses evoked at a matching depolarized membrane potential (Fig. 2A, pulse: $F_{(1,6)} = 41.12$; $p = 0.001$, ANOVA); however, the amplitude of HP2 responses changed in the presence of PTX (drug $\times$ pulse: $F_{(1,6)} = 8.35$; $p = 0.028$, ANOVA). Specifically, the magnitude of HP2 suppression driven by PFC stimulation was greatly reduced in the presence of PTX compared with vehicle conditions, similar to previous *in vivo* findings. With GABA$_A$Rs blocked, PFC stimulation reduced HP2 EPSP amplitudes by 33.8 ± 18.7% compared with a 52.2 ± 17.6% reduction observed in the absence of PTX (Fig. 2B; $t_{(6)} = 4.17$; $p = 0.006$, paired t test). This reduction was not due to any changes to HP1 EPSP amplitude following PTX administration ($t_{(6)} = 1.98$; $p = 0.095$, paired t test). As the reduction was not completely reversed by PTX, it is likely that other mechanisms contribute to PFC-evoked heterosynaptic suppression.

GABA$_B$Rs are also found throughout the VS (Bowery et al., 1987) and can inhibit presynaptic glutamate release in mice (Tejeda et al., 2017). It is possible that the local inhibitory signal recruited by robust PFC stimulation could activate both GABA$_A$Rs and GABA$_B$Rs. To test for a role of GABA$_B$Rs in heterosynaptic suppression in the VS, we measured MSN responses to HP stimulation in the presence of the GABA$_B$R antagonist SAC (10 μM; $n = 6$ cells/5 rats). Similar to PTX, HP2 responses evoked at the
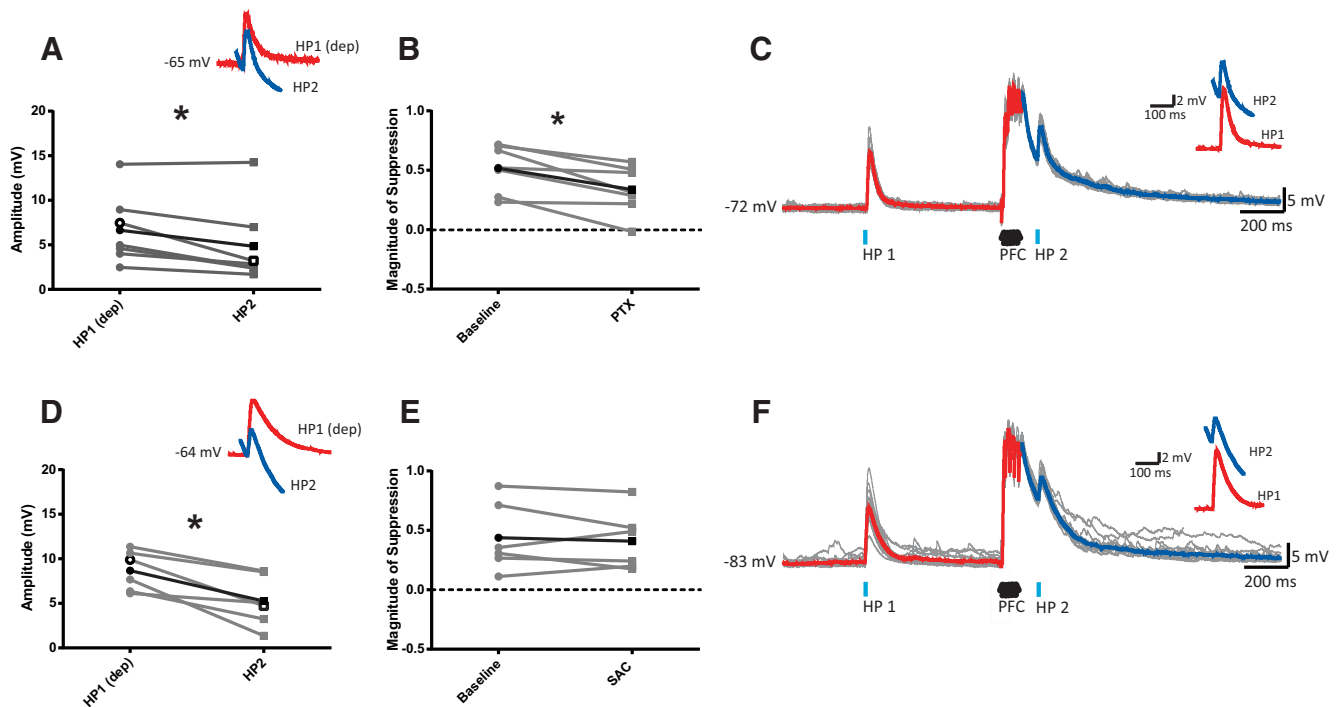
Figure 2. Blockade of GABA$_A$Rs, but not GABA$_B$Rs, attenuates PFC-evoked heterosynaptic suppression of HP inputs to the VS. **A**, Averaged EPSP amplitudes for individual MSNs treated with PTX (100 μM) showing that HP2 EPSPs are reduced compared with HP1 responses evoked at a similar membrane potential. Inset, Averaged depolarized HP1 and basal HP2 EPSPs in the same representative cell. **B**, Plot comparing the magnitude of HP2 suppression driven by PFC stimulation under baseline conditions and in the presence of PTX for individual MSNs. Blockade of GABA$_A$Rs reduced the extent of HP2 heterosynaptic suppression induced by PFC stimulation. **C**, Traces showing response to optogenetic stimulation of HP terminals before (HP1) and 50 ms after (HP2) PFC train stimulation in a representative MSN treated with PTX. Averaged responses to HP1 and HP2 (highlighted in red and blue, respectively) are overlaid in the inset (average of 15 sweeps; gray). **D**, EPSP amplitudes for individual MSNs treated with SAC (10 μM) showing that HP2 EPSPs are significantly reduced compared with HP1 responses evoked at a similar membrane potential. **E**, Plot comparing the magnitude of HP2 suppression driven by PFC stimulation under baseline conditions and in the presence of SAC for individual MSNs. No change in suppression was observed following blockade of GABA$_B$Rs. **F**, Responses to optogenetic stimulation of HP terminals before (HP1) and 50 ms after (HP2) PFC train stimulation in a representative MSN treated with SAC. *$p < 0.05$.

50 ms delay period remained significantly reduced compared with baseline HP1 responses following administration of SAC (Fig. 2D, pulse: $F_{(1,5)} = 13.26$; $p = 0.015$, ANOVA). Unlike GABA$_A$Rs, however, the blockade of GABA$_B$Rs had no effect on the magnitude of suppression recorded (Fig. 2E; $t_{(5)} = 0.31$; $p = 0.768$, paired t test), suggesting that GABA$_B$Rs do not contribute to PFC-evoked heterosynaptic suppression. Thus, these data confirm and extend previous *in vivo* data suggesting that GABA$_A$-mediated inhibition contributes to the suppression of HP responses onto VS MSNs following burst-like PFC stimulation.

Selective recruitment of KOR signaling in striatal heterosynaptic suppression

The observation that direct blockade of GABA$_A$Rs only partially restored PFC-induced suppression of HP inputs suggests that heterosynaptic suppression in the VS is a complex process involving multiple mechanisms. Inhibition of presynaptic excitatory neurotransmission through KOR/DYN signaling could contribute to this phenomenon. Several studies have demonstrated that activation of presynaptic KORs reduces glutamate release in the VS (Hjelmstad and Fields, 2001, 2003; Tejeda et al., 2017). To determine whether KOR activation modulates specific glutamatergic inputs onto striatal MSNs, the effect of a selective KOR agonist, U69,593 (1 μM), on HP- and PFC-specific EPSPs was examined in the same MSN ($n = 8$ cells/5 rats). Overall, U69,593 significantly reduced the amplitude of HP- and PFC-evoked responses (Fig. 3A; treatment: $F_{(1,7)} = 27.58$, $p = 0.001$, ANOVA). KOR modulation of synaptic responses did not significantly differ between inputs (treatment × input: $F_{(1,7)} = 3.41$, $p = 0.107$,

ANOVA), with U69,593 administration decreasing HP and PFC EPSP amplitudes by ~36% (from 13.8 ± 6.3 mV to 9.1 ± 5.7 mV; $t_{(7)} = 3.95$, $p = 0.006$, paired t test; Fig. 3B) and ~21% (from 14.1 ± 3.0 mV to 11.5 ± 3.8 mV; $t_{(7)} = 7.12$, $p = 0.001$, paired t test; Fig. 3C), respectively. Thus, these data suggest that KOR activation affects both PFC and HP inputs to the VS in rats.

To assess the possible contribution of KOR activation during PFC-induced heterosynaptic suppression, MSN responses to the HP1-PFC-HP2 protocol were measured in the presence of the KOR antagonist norBNI (100 nM; $n = 9$ cells/7 rats). Following norBNI bath application, HP2 responses evoked 50 ms after PFC stimulation remained reduced relative to membrane potential-matched HP1 responses (Fig. 3D; pulse: $F_{(1,8)} = 59.48$; $p = 0.001$, ANOVA). However, the magnitude of suppression changed significantly in response to drug application (drug × pulse: $F_{(1,8)} = 7.48$; $p = 0.026$, ANOVA). In the absence of norBNI, PFC stimulation reduced HP2-evoked responses by $40.8 \pm 14.3\%$, but this decreased to $17.5 \pm 21.6\%$ following bath application of norBNI (Fig. 3E; $t_{(8)} = 2.859$; $p = 0.021$, paired t test). Furthermore, this reduction was not the result of a change in HP1 EPSP amplitudes following norBNI administration ($t_{(8)} = 1.50$; $p = 0.173$, paired t test). These data suggest that KOR activation plays a key role in PFC-induced heterosynaptic suppression in the VS.

It is likely that both GABA$_A$Rs and KORs contribute to VS heterosynaptic suppression following robust PFC stimulation. Either GABA$_A$R or KOR blockade was capable of diminishing the amount of suppression driven by PFC stimulation, but neither drug alone was able to completely reverse these effects. It is possible that both mechanisms work simultaneously to induce sup-
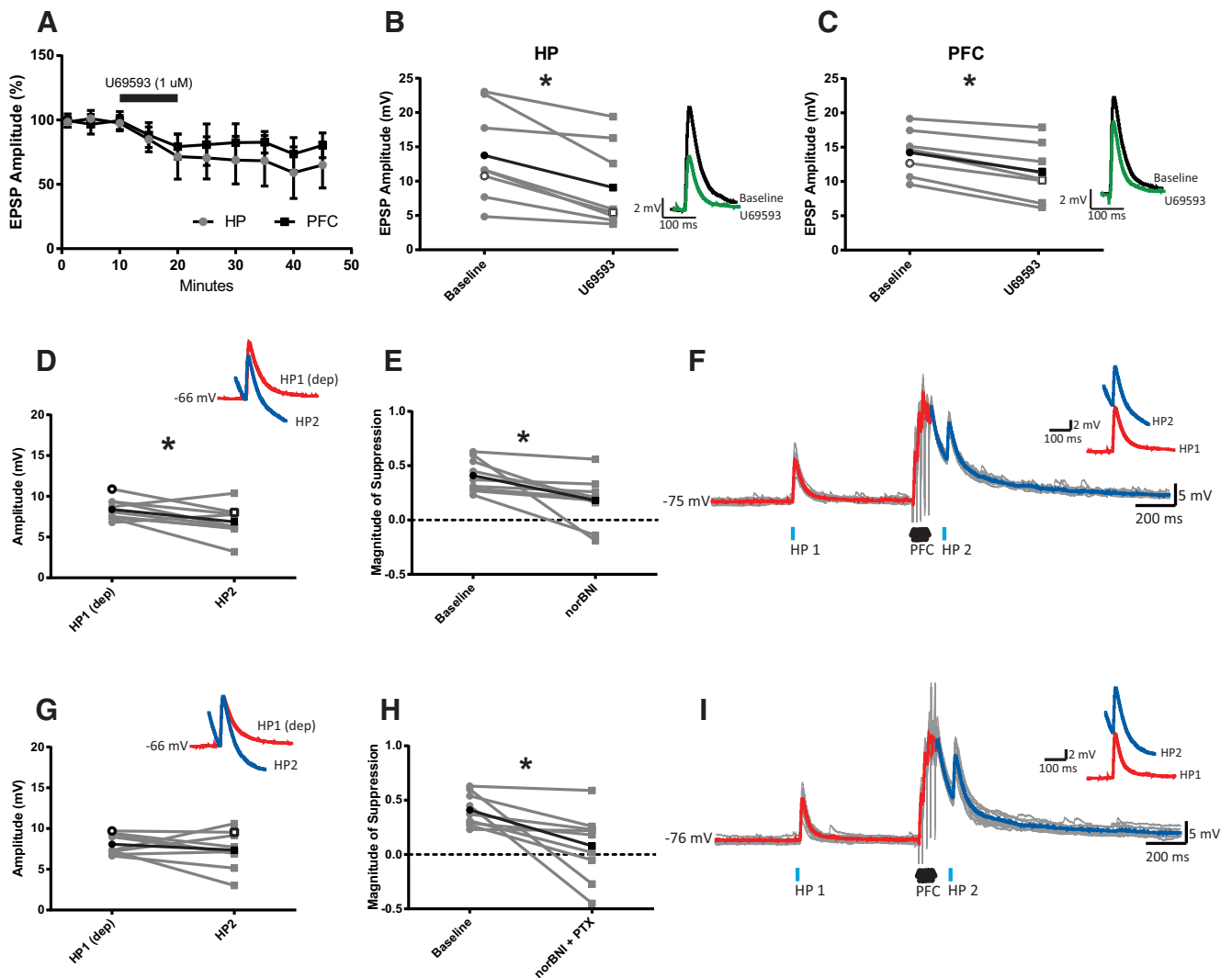
Figure 3. Combined antagonism of GABA$_A$Rs and KORs blocks heterosynaptic suppression of HP inputs in the VS. ***A***, Group data of HP and PFC EPSP amplitudes averaged over 5 min. Bath application of U69,593 (1 μM) significantly reduced the amplitude of HP- and PFC-evoked responses. Black bar represents the duration of drug application. ***B***, Plot comparing EPSP amplitudes evoked by HP stimulation under baseline and U69,593 conditions for individual MSNs. Values represent the average of the last 5 min of baseline compared with the last 5 min of the recording session (and in Fig. 4). Inset, Representative EPSPs evoked under baseline (black) and U69,593 conditions (green) are overlaid. Open black symbols represent corresponding data. Closed black symbols represent group averages. ***C***, Plot comparing EPSP amplitudes evoked by single-pulse PFC stimulation under baseline and U69,593 conditions. ***D***, Averaged EPSP amplitudes for individual MSNs treated with norBNI (100 nM) showing that HP2 EPSPs are still significantly reduced compared with HP1 responses evoked at a similar membrane potential. Inset, Averaged depolarized HP1 and basal HP2 EPSPs in the same representative cell. ***E***, Plot comparing the magnitude of HP2 suppression driven by PFC stimulation under baseline conditions and in the presence of norBNI for individual MSNs. Blockade of κ opioid receptors reduced the extent of HP2 heterosynaptic suppression induced by PFC stimulation. ***F***, Responses to optogenetic stimulation of HP terminals before (HP1) and 50 ms after (HP2) PFC train stimulation in a representative MSN treated with norBNI. Inset, Averaged responses to HP1 and HP2 (highlighted in red and blue, respectively) are overlaid (average of 15 sweeps; gray). ***G***, Averaged EPSP amplitudes for individual MSNs treated with norBNI (100 nM) and PTX (100 μM) showing that HP1 and HP2 responses do not differ compared at a similar membrane potential. ***H***, Plot comparing the magnitude of HP2 suppression driven by PFC stimulation under baseline conditions and in the presence of norBNI and PTX for individual MSNs. Blockade of GABA$_A$Rs and KORs reversed the heterosynaptic suppression of HP2 responses by PFC stimulation. ***I***, Responses to optogenetic stimulation of HP terminals before (HP1) and 50 ms after (HP2) PFC train stimulation in a representative MSN treated with norBNI and PTX. *$p < 0.05$.

pression following robust PFC stimulation. Coadministration of norBNI (100 nM) and PTX (100 μM) significantly blocked the attenuation of HP2 responses (drug $\times$ pulse: $F_{(1,8)} = 10.16$; $p = 0.013$, ANOVA). HP2-evoked EPSP amplitudes were not significantly different from HP1 responses (Fig. 3G; $t_{(8)} = 0.93$; $p = 0.381$, paired t test), and the magnitude of HP2 suppression decreased significantly from 40.8 $\pm$ 14.3% during baseline recordings to 8.0 $\pm$ 29.1% with norBNI and PTX coadministration (Fig. 3H; $t_{(8)} = 3.00$; $p = 0.018$, paired t test). It should be noted that HP1 amplitude decreased from 9.2 $\pm$ 1.1 mV to 8.1 $\pm$ 1.1 mV following bath application of norBNI and PTX ($t_{(8)} = 3.00$; $p = 0.018$, paired t test), indicating that the combination of

norBNI and PTX could impact HP synaptic activity independently of PFC stimulation. However, it is unlikely that this modest change in amplitude is solely responsible for driving the effects reported above as a similar decrease in EPSP amplitude was not seen for HP2-evoked responses. Thus, these data suggest that burst-like PFC activity elicits brief heterosynaptic suppression of HP inputs to the VS through the combined activation of GABA$_A$R and KOR signaling.

There are other retrograde signaling mechanisms in the VS that could contribute to PFC-evoked heterosynaptic suppression. For example, endocannabinoids are also synthesized and released from MSN, and signaling via their endogenous receptor, the cannabinoid 1 receptor (CB1), has also been shown to reduce
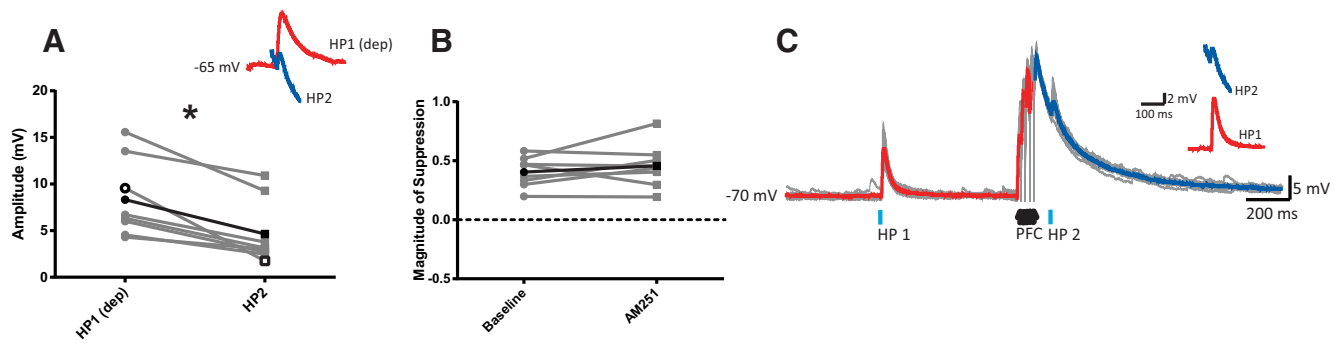
Figure 4. Cortically induced heterosynaptic suppression of HP responses in the VS does not involve CB1 receptor activation. **A**, Averaged EPSP amplitudes for individual MSNs treated with AM251 (2 μM) showing that HP2 EPSPs are significantly reduced compared with HP1 responses evoked at a similar membrane potential. Inset, Averaged depolarized HP1 and basal HP2 EPSPs in the same representative cell. **B**, Plot comparing the magnitude of HP2 suppression driven by PFC stimulation under baseline conditions and in the presence of AM251 for individual MSNs. No change in suppression was observed following blockade of CB1 receptors. **C**, Responses to optogenetic stimulation of HP terminals before (HP1) and 50 ms after (HP2) PFC train stimulation in a representative MSN treated with AM251. Averaged responses to HP1 and HP2 (highlighted in red and blue, respectively) are overlaid in the inset (average of 15 sweeps; gray). *$p < 0.05$.

presynaptic glutamate release (Gerdeman and Lovinger, 2001; Hoffman and Lupica, 2001). An evaluation of CB1 receptors in cortically induced heterosynaptic suppression by bath application of the CB1 receptor antagonist AM251 (2 μM; $n = 8$ cells/5 rats) revealed that HP2 responses remained significantly reduced compared with HP1 (Fig. 4A, pulse: $F_{(1,7)} = 34.35$; $p = 0.001$, ANOVA). The magnitude of suppression also remained unchanged compared with baseline (Fig. 4B; $t_{(7)} = 1.03$; $p = 0.339$, paired t test), suggesting that CB1 receptors do not contribute to PFC-evoked heterosynaptic suppression.

Discussion

Burst-like stimulation of corticostriatal fiber tracts suppressed optogenetically evoked HP responses in VS MSNs recorded in acute adult rat slices. Heterosynaptic suppression was greatest following a short latency after PFC burst stimulation. Cortical stimulation was required for HP suppression, as no change in HP response was observed in the absence of PFC activation. Heterosynaptic suppression was not a result of the transient depolarization induced by PFC stimulation. Rather, the blockade of GABA$_A$Rs, but not GABA$_B$Rs, led to a partial reduction in the magnitude of PFC-evoked suppression. A similar reduction in heterosynaptic suppression was observed in the presence of the KOR antagonist, norBNI. Finally, near-complete blockade of PFC-induced heterosynaptic suppression was achieved through the combined administration of both GABA$_A$R and KOR antagonists. These data support the assertion that high-frequency PFC stimulation suppresses competing excitatory inputs onto striatal MSNs through activation of presynaptic and postsynaptic signaling mechanisms.

GABAergic and KOR mechanisms underlie cortical heterosynaptic suppression of HP inputs to the VS
PTX administration reduced the extent of PFC-induced heterosynaptic suppression of HP inputs onto VS MSNs. This observation is consistent with previous *in vivo* reports (Calhoon and O'Donnell, 2013) using intracellular methods of GABA$_A$R antagonism. These data suggest that robust PFC activation engages local inhibitory mechanisms to suppress the synaptic efficacy of competing excitatory inputs onto MSNs. However, the source of inhibition is not clear. Striatal inhibition can arise from GABAergic interneurons, as well as collaterals from neighboring MSNs (Kita, 1993). Despite dense local collaterals, electrophysiological studies indicate only a weak connection between neighboring MSNs (Jaeger et al., 1994; Guzmán et al., 2003; Koos et al., 2004;

Taverna et al., 2004). Conversely, fast-spiking interneurons (FSIs) immunoreactive for the calcium binding protein, parvalbumin, provide selective and powerful feedforward inhibitory control over MSN activity through perisomatic inhibition (Kita et al., 1990; Bennett and Bolam, 1994; Koós and Tepper, 1999). Activation of these inputs is sufficient to delay or block MSN excitation and is predominantly mediated by GABA$_A$Rs (Koos et al., 2004; Szydlowski et al., 2013). Furthermore, corticostriatal inputs are known to provide dense, monosynaptic input to striatal FSI, and burst-like stimulation of PFC inputs results in activation of this cell population (Mallet et al., 2005; Gruber et al., 2009b). GABAergic interneurons are thought to form a critical link in mediating corticostriatal feedforward inhibition. Thus, it is likely that GABAergic inhibition recruited during high-frequency PFC stimulation of the VS is derived primarily from cortical activation of local FSI interneurons.

In addition to local inhibitory mechanisms, these data indicate that KOR signaling also plays a role in PFC-induced heterosynaptic suppression as local blockade of KORs greatly reduced the magnitude of suppression. Our results are consistent with an inhibitory role of KOR on synaptic excitatory transmission and likely reflect a presynaptic decrease in glutamate release. KOR immunoreactivity has been reported in asymmetric synapses within the VS (Svingos et al., 1999), and activation of these receptors either decreases Ca^{2+} channel conductance or activates inward-rectifying K$^+$ channels (Tallent et al., 1994; Al-Hasani and Bruchas, 2011), inhibiting presynaptic release of excitatory neurotransmitter (Hjelmstad and Fields, 2001). In support of this assertion, we found that the KOR agonist U69,593 significantly reduced HP- and PFC-evoked synaptic responses in recorded MSNs. Recent work (Tejeda et al., 2017) indicates that KOR activation may confer pathway specificity by selectively modulating BLA excitatory input onto D1 MSNs. However, they did not observe KOR-mediated inhibition of HP glutamate release in the mouse VS. This discrepancy could be indicative of species differences in KOR expression or afferent innervation patterns. Indeed, varied distribution of opioid receptors has been reported across multiple rodent species (McLean et al., 1987; Rácz and Halasy, 2003). Conflicting results could also be due to differences in viral injection and/or recording sites. To ensure robust ChR2 expression throughout the VS, we used a multisite injection protocol, which consistently transfected a large region of the ventral HP along the septal-temporal axis. This injection pattern, cou-

pled with a sagittal slice preparation, permitted MSN recording across all subdivisions of the VS along the rostrocaudal axis. Thus, KOR activity can modulate both HP and PFC inputs in the VS, and strong PFC activation can drive KOR- and GABA$_A$R-dependent heterosynaptic suppression in the VS.

It could be hypothesized that the changes in heterosynaptic suppression observed following norBNI administration are the indirect result of KOR modulation of mesolimbic DA release. In addition to excitatory neurotransmission, the KOR system plays an important role in the modulation of mesolimbic DA release. Striatal KORs are also localized on DA varicosities (Meshul and McGinty, 2000), and administration of KOR antagonists leads to increased DA levels in this region (Maisonneuve et al., 1994). Similar to KOR, DA inhibits striatal glutamatergic transmission through modulation of presynaptic excitatory inputs to the VS (Pennartz et al., 1992; O'Donnell and Grace, 1994; Nicola et al., 1996). However, it is unlikely that DA plays a role in the KOR-dependent effects we observed because blockade of D1 and D2 receptors through the coadministration of SCH-23390 and sulpiride has no effect on the inhibition of excitatory synaptic potentials produced by U69,593 (Hjelmstad and Fields, 2001).

A more parsimonious model suggests that robust PFC afferent activation results in postsynaptic DYN release, which, in turn, attenuates ongoing signaling from competing afferents through activation of presynaptic KORs. The neuropeptide DYN is the endogenous ligand of the KORs (Chavkin et al., 1982). Colabeling studies in the VS show that KOR-immunoreactive terminals are in close opposition to DYN-containing MSNs (Svingos et al., 1999). Although the mechanisms leading to DYN release remain unclear, it has been hypothesized that postsynaptic DYN release requires robust or repetitive excitatory stimulation of the target neuron (Seward et al., 1995), similar to other neuropeptides. In support of this assertion, endogenous DYN release has been observed in the HP (Wagner et al., 1990) and VS (Al-Hasani et al., 2015) in response to 10–50 Hz, high-intensity stimulation, similar to that used in the present study.

It should be noted that high-frequency stimulation of the corticostriatal pathway can induce postsynaptic release of several signaling molecules within the VS. For example, postsynaptic MSN release of endocannabinoids relies heavily on robust or repetitive excitatory afferent activity (Adermark and Lovinger, 2007). Upon release, endocannabinoids bind to CB1 receptors present, in large part, on presynaptic terminals forming excitatory, asymmetric synapses (Svingos et al., 1999). Activation of CB1 receptors has also been shown to decrease presynaptic glutamate release in the VS (Gerdeman and Lovinger, 2001; Hoffman and Lupica, 2001). However, we found that bath application of the CB1 receptor antagonist AM251 had no impact on the magnitude of PFC-induced HP suppression.

Functional implication of cortical heterosynaptic suppression in the VS

The PFC, HP, and VS make up a highly integrated and dynamic neural system responsible for generating motivated behavior, with each region providing critical information used to guide response selection. Hippocampal inputs mediate context-related behaviors, whereas the information passed within the PFC-VS circuit supports rapid adaption of appropriate behavioral strategies in response to dynamic changes in task requirements (Block et al., 2007). As the point of convergence, the VS is proposed to play the role of a "behavioral switchboard," allowing flexible selection of afferent input to drive MSN ensemble activity depending on the behavioral state of the subject (Gruber et al., 2009a). In

keeping with this conceptualization of striatal information processing, our data allow us to hypothesize that brief heterosynaptic suppression driven by strong PFC activation facilitates the efficient transfer of cortical information through the VS during critical decision-making instances. As such, cortical recruitment of KORs and GABA$_A$Rs would serve to enhance the throughput of salient cortical information by dampening competing information from weaker inputs. This could occur through KOR-mediated decrease in excitatory drive onto D1 MSNs and concurrent disinhibition of D2 MSNs (Tejeda et al., 2017), thus dynamically altering ensemble-based activity in the direct and indirect output pathways of the striatum and aiding changes in action selection and initiation.

Future experiments should be directed at understanding the impact of these mechanisms on behavior. The transient nature of this suppression suggests that it may be critical for effective information integration by ensuring minimal disruption to information flow from other limbic inputs. Thus, loss of temporal resolution in these nonlinear interactions could underlie some of the maladaptive behaviors associated with many neurological disorders. For example, excessive corticostriatal activity could lead to enhanced FSI feedforward inhibition or DYN release that would interfere with the transfer of information from noncortical regions necessary to update or change behavioral strategies. This condition would obscure the "behavioral switchboard" function of the VS, yielding behavioral inflexibility. Indeed, pathophysiological changes in PFC-VS interactions and KOR activity have been implicated in several neurological and psychiatric disorders, including schizophrenia (O'Donnell and Grace, 1999; Meyer-Lindenberg et al., 2002) and drug addiction (Kalivas and Volkow, 2005). As these conditions may be marked by aberrant motivational states and inflexible behavior, it is possible that modulating KOR-dependent local interactions could aid in reversing those deficits.

References

Adermark L, Lovinger DM (2007) Retrograde endocannabinoid signaling at striatal synapses requires a regulated postsynaptic release step. Proc Natl Acad Sci U S A 104:20564–20569. CrossRef Medline

Al-Hasani R, Bruchas MR (2011) Molecular mechanisms of opioid receptor-dependent signaling and behavior. Anesthesiology 115:1363–1381. CrossRef Medline

Al-Hasani R, McCall JG, Shin G, Gomez AM, Schmitz GP, Bernardi JM, Pyo CO, Park SI, Marcinkiewcz CM, Crowley NA, Krashes MJ, Lowell BB, Kash TL, Rogers JA, Bruchas MR (2015) Distinct subpopulations of nucleus accumbens dynorphin neurons drive aversion and reward. Neuron 87:1063–1077. CrossRef Medline

Altar CA, Hauser K (1987) Topography of substantia nigra innervation by D1 receptor-containing striatal neurons. Brain Res 410:1–11. CrossRef Medline

Bennett BD, Bolam JP (1994) Synaptic input and output of parvalbumin-immunoreactive neurons in the neostriatum of the rat. Neuroscience 62:707–719. CrossRef Medline

Berendse HW, Galis-de Graaf Y, Groenewegen HJ (1992) Topographical organization and relationship with ventral striatal compartments of prefrontal corticostriatal projections in the rat. J Comp Neurol 316:314–347. CrossRef Medline

Block AE, Dhanji H, Thompson-Tardif SF, Floresco SB (2007) Thalamic-prefrontal cortical-ventral striatal circuitry mediates dissociable components of strategy set shifting. Cereb Cortex 17:1625–1636. CrossRef Medline

Bowery NG, Hudson AL, Price GW (1987) GABAA and GABAB receptor site distribution in the rat central nervous system. Neuroscience 20:365–383. CrossRef Medline

Calhoon GG, O'Donnell P (2013) Closing the gate in the limbic striatum: prefrontal suppression of hippocampal and thalamic inputs. Neuron 78:181–190. CrossRef Medline

Chavkin C, James IF, Goldstein A (1982) Dynorphin is a specific endoge-

nous ligand of the kappa opioid receptor. Science 215:413–415. CrossRef Medline

Di Chiara G, Imperato A (1988) Opposite effects of mu and kappa opiate agonists on dopamine release in the nucleus accumbens and in the dorsal caudate of freely moving rats. J Pharmacol Exp Ther 244:1067–1080. Medline

Ebner SR, Roitman MF, Potter DN, Rachlin AB, Chartoff EH (2010) Depressive-like effects of the kappa opioid receptor agonist salvinorin A are associated with decreased phasic dopamine release in the nucleus accumbens. Psychopharmacology (Berl) 210:241–252. CrossRef Medline

Fallon JH, Leslie FM (1986) Distribution of dynorphin and enkephalin peptides in the rat brain. J Comp Neurol 249:293–336. CrossRef Medline

French SJ, Totterdell S (2002) Hippocampal and prefrontal cortical inputs monosynaptically converge with individual projection neurons of the nucleus accumbens. J Comp Neurol 446:151–165. CrossRef Medline

Gerdeman G, Lovinger DM (2001) CB1 cannabinoid receptor inhibits synaptic release of glutamate in rat dorsolateral striatum. J Neurophysiol 85:468–471. Medline

Groenewegen HJ, Mulder AB, Beijer AV, Wright CI, Lopes da Silva FH, Pennartz CM (1999) Hippocampal and amygdaloid interactions in the nucleus accumbens. Psychobiology 27:149–164.

Gruber AJ, Hussain RJ, O'Donnell P (2009a) The nucleus accumbens: a switchboard for goal-directed behaviors. PLoS One 4:e5062. CrossRef Medline

Gruber AJ, Powell EM, O'Donnell P (2009b) Cortically activated interneurons shape spatial aspects of cortico-accumbens processing. J Neurophysiol 101:1876–1882. CrossRef Medline

Guzmán JN, Hernández A, Galarraga E, Tapia D, Laville A, Vergara R, Aceves J, Bargas J (2003) Dopaminergic modulation of axon collaterals interconnecting spiny neurons of the rat striatum. J Neurosci 23:8931–8940. Medline

Hill MP, Brotchie JM (1999) Control of glutamate release by calcium channels and kappa-opioid receptors in rodent and primate striatum. Br J Pharmacol 127:275–283. CrossRef Medline

Hjelmstad GO, Fields HL (2001) Kappa opioid receptor inhibition of glutamatergic transmission in the nucleus accumbens shell. J Neurophysiol 85:1153–1158. Medline

Hjelmstad GO, Fields HL (2003) Kappa opioid receptor activation in the nucleus accumbens inhibits glutamate and GABA release through different mechanisms. J Neurophysiol 89:2389–2395. CrossRef Medline

Hoffman AF, Lupica CR (2001) Direct actions of cannabinoids on synaptic transmission in the nucleus accumbens: a comparison with opioids. J Neurophysiol 85:72–83. Medline

Jaeger D, Kita H, Wilson CJ (1994) Surround inhibition among projection neurons is weak or nonexistent in the rat neostriatum. J Neurophysiol 72:2555–2558. Medline

Kalivas PW, Volkow ND (2005) The neural basis of addiction: a pathology of motivation and choice. Am J Psychiatry 162:1403–1413. CrossRef Medline

Kita H (1993) GABAergic circuits of the striatum. In: Chemical signaling in the basal ganglia (Arbuthnott GW, Emson PC, eds). Amsterdam: Elsevier.

Kita H, Kosaka T, Heizmann CW (1990) Parvalbumin-immunoreactive neurons in the rat neostriatum: a light and electron microscopic study. Brain Res 536:1–15. CrossRef Medline

Koós T, Tepper JM (1999) Inhibitory control of neostriatal projection neurons by GABAergic interneurons. Nat Neurosci 2:467–472. CrossRef Medline

Koos T, Tepper JM, Wilson CJ (2004) Comparison of IPSCs evoked by spiny and fast-spiking neurons in the neostriatum. J Neurosci 24:7916–7922. CrossRef Medline

Maisonneuve IM, Archer S, Glick SD (1994) U50,488, a kappa opioid receptor agonist, attenuates cocaine-induced increases in extracellular dopamine in the nucleus accumbens of rats. Neurosci Lett 181:57–60. CrossRef Medline

Mallet N, Le Moine C, Charpier S, Gonon F (2005) Feedforward inhibition of projection neurons by fast-spiking GABA interneurons in the rat striatum in vivo. J Neurosci 25:3857–3869. CrossRef Medline

Mansour A, Fox CA, Burke S, Meng F, Thompson RC, Akil H, Watson SJ (1994) Mu, delta, and kappa opioid receptor mRNA expression in the rat CNS: an in situ hybridization study. J Comp Neurol 350:412–438. CrossRef Medline

McLean S, Rothman RB, Jacobson AE, Rice KC, Herkenham M (1987) Distribution of opiate receptor subtypes and enkephalin and dynorphin immunoreactivity in the hippocampus of squirrel, guinea pig, rat, and hamster. J Comp Neurol 255:497–510. CrossRef Medline

Meshul CK, McGinty JF (2000) Kappa opioid receptor immunoreactivity in the nucleus accumbens and caudate-putamen is primarily associated with synaptic vesicles in axons. Neuroscience 96:91–99. CrossRef Medline

Meyer-Lindenberg A, Miletich RS, Kohn PD, Esposito G, Carson RE, Quarantelli M, Weinberger DR, Berman KF (2002) Reduced prefrontal activity predicts exaggerated striatal dopaminergic function in schizophrenia. Nat Neurosci 5:267–271. CrossRef Medline

Nicola SM, Kombian SB, Malenka RC (1996) Psychostimulants depress excitatory synaptic transmission in the nucleus accumbens via presynaptic D1-like dopamine receptors. J Neurosci 16:1591–1604. Medline

O'Donnell P, Grace AA (1994) Tonic D_2-mediated attenuation of cortical excitation in nucleus accumbens neurons recorded in vitro. Brain Res 634:105–112. CrossRef Medline

O'Donnell P, Grace AA (1995) Synaptic interactions among excitatory afferents to nucleus accumbens neurons: hippocampal gating of prefrontal cortical input. J Neurosci 15:3622–3639. Medline

O'Donnell P, Grace A (1999) Disruption of information flow within cortical-limbic circuits and the pathophysiology of schizophrenia. In: Schizophrenia in a molecular age (Tamminga CA, ed), pp 109–140. Washington, DC: American Psychiatric.

Pennartz CM, Dolleman-Van der Weel MJ, Kitai ST, Lopes da Silva FH (1992) Presynaptic dopamine D_1 receptors attenuate excitatory and inhibitory limbic inputs to the shell region of the rat nucleus accumbens. J Neurophysiol 67:1325–1334. Medline

Rácz B, Halasy K (2003) Kappa-opioid receptor in the rodent hippocampus: a comparative immunocytochemical study in the rat, guinea pig, hamster and gerbil. Acta Biol Hung 54:45–53. Medline

Rawls SM, McGinty JF (1998) Kappa receptor activation attenuates L-trans-pyrrolidine-2,4-dicarboxylic acid-evoked glutamate levels in the striatum. J Neurochem 70:626–634. CrossRef Medline

Rawls SM, McGinty JF, Terrian DM (1999) Presynaptic kappa-opioid and muscarinic receptors inhibit the calcium-dependent component of evoked glutamate release from striatal synaptosomes. J Neurochem 73:1058–1065. CrossRef Medline

Seward EP, Chernevskaya NI, Nowycky MC (1995) Exocytosis in peptidergic nerve terminals exhibits two calcium-sensitive phases during pulsatile calcium entry. J Neurosci 15:3390–3399. Medline

Spanagel R, Herz A, Shippenberg TS (1992) Opposing tonically active endogenous opioid systems modulate the mesolimbic dopaminergic pathway. Proc Natl Acad Sci U S A 89:2046–2050. CrossRef Medline

Svingos AL, Colago EE, Pickel VM (1999) Cellular sites for dynorphin activation of k-opioid receptors in the rat nucleus accumbens shell. J Neurosci 19:1804–1813. Medline

Szydlowski SN, Pollak Dorocic I, Planert H, Carlén M, Meletis K, Silberberg G (2013) Target selectivity of feedforward inhibition by striatal fast-spiking interneurons. J Neurosci 33:1678–1683. CrossRef Medline

Tallent M, Dichter MA, Bell GI, Reisine T (1994) The cloned kappa opioid receptor couples to an N-type calcium current in undifferentiated PC-12 cells. Neuroscience 63:1033–1040. CrossRef Medline

Taverna S, van Dongen YC, Groenewegen HJ, Pennartz CM (2004) Direct physiological evidence for synaptic connectivity between medium-sized spiny neurons in rat nucleus accumbens in situ. J Neurophysiol 91:1111–1121. Medline

Tejeda HA, Wu J, Kornspun AR, Pignatelli M, Kashtelyan V, Krashes MJ, Lowell BB, Carlezon WA Jr, Bonci A (2017) Pathway- and cell-specific kappa-opioid receptor modulation of excitation-inhibition balance differentially gates D1 and D2 accumbens neuron activity. Neuron 93:147–163. CrossRef Medline

Wagner JJ, Caudle RM, Neumaier JF, Chavkin C (1990) Stimulation of endogenous opioid release displaces mu receptor binding in rat hippocampus. Neuroscience 37:45–53. CrossRef Medline